Kidney International, Vol. 66 (2004), pp. 1272–1278

TECHNICAL NOTE

Free-breathing renal MR angiography with steady-state free-precession (SSFP) and slab-selective spin inversion: Initial results

MARCUS KATOH, ARNO BUECKER, MATTHIAS STUBER, ROLF W. GÜNTHER, and ELMAR SPUENTRUP

Department of Diagnostic Radiology, University Hospital, University of Technology, Aachen, Germany; and Johns Hopkins University School of Medicine, Baltimore, Maryland

Free-breathing renal MR angiography with steady-state free-precession (SSFP) and slab-selective spin inversion: Initial results.

Background. The aim of our study was the investigation of a novel navigator-gated three-dimensional (3D) steady-state free-precession (SSFP) sequence for free-breathing renal magnetic resonance angiography (MRA) without contrast medium, and to examine the advantage of an additional inversion prepulse for improved contrast.

Methods. Eight healthy volunteers (mean age 29 years) and eight patients (mean age 53 years) were investigated on a 1.5 Tesla MR system (ACS-NT, Philips, Best, The Netherlands). Renal MRA was performed using three navigator-gated free-breathing cardiac-triggered 3D SSFP sequences [repetition time (TR) = 4.4 ms, echo time (TE) = 2.2 ms, flip angle 85°, spatial resolution 1.25 × 1.25 × 4.0 mm^3, scanning time approximately 1 minute 30 seconds]. The same sequence was performed without magnetization preparation, with a non-slab selective and a slab-selective inversion prepulse. Signal-to-noise ratio (SNR), contrast-to-noise (CNR) vessel length, and subjective image quality were compared.

Results. Three-dimensional SSFP imaging combined with a slab-selective inversion prepulse enabled selective and high contrast visualization of the renal arteries, including the more distal branches. Standard SSFP imaging without magnetization preparation demonstrated overlay by veins and renal parenchyma. A non–slab-selective prepulse abolished vessel visualization. CNR in SSFP with slab-selective inversion was 43.6 versus 10.6 (SSFP without magnetization preparation) and 0.4 (SSFP with non–slab-selective inversion), $P < 0.008$.

Conclusion. Navigator-gated free-breathing cardiac-triggered 3D SSFP imaging combined with a slab-selective inversion prepulse is a novel, fast renal MRA technique without the need for contrast media.

Key words: renal MR angiography, steady-state free-precession (SSFP), slab-selective inversion prepulse.

Received for publication January 7, 2004
and in revised form March 18, 2004
Accepted for publication April 2, 2004

Several magnetic resonance angiographic techniques with fundamentally different image contrast mechanisms have been implemented for noninvasive imaging of the renal arteries. These include time-of-flight [1–3] and phase-contrast [4, 5] magnetic resonance angiography (MRA). Though considered to provide accurate images of normal arteries, the use of these techniques tends to result in overestimation of stenotic lesions due to artifacts caused by turbulent flow [6]. Furthermore, depiction of distal arteries is limited. Subsequently, three-dimensional (3D) contrast-enhanced MRA (ceMRA) has become the gold standard for MRA of the renal arteries [5]. Contrast is based on the T_1-shortening of blood due to contrast media, which is independent of inflow effects. For high contrast between arteries and surrounding tissue, data acquisition has to be performed during the first pass of the contrast medium [7]. A short acquisition window and optimal bolus timing is crucial to avoid venous signal enhancement [8]. The technique is typically performed during one breath-hold, which limits spatial resolution [9]. Moreover, image quality is impaired because no cardiac triggering can be applied, resulting in blurring due to the aortic pulse wave [10]. Over the last decade other alternative renal MRA techniques like the Echo-planar imaging-signal targeting with alternating radiofrequency (EPI-STAR) [11, 12] or the projection MRA using aortic spin labeling [13] have been implemented, which provide excellent background suppression and high-contrast visualization of the renal arteries. Hereby, contrast is based on the altered net magnetization of the inflowing blood into the imaging volume after tagging. Both techniques require the acquisition of two data sets, which finally have to be added or subtracted to or from each other, thus bearing the potential of addition or subtraction artifacts. While EPI-STAR is performed during breath-hold, the spin labeling technique described by Spuentrup et al [13] requires a significantly prolonged scanning time due to the two data sets.

The purpose of our study was to implement a faster renal MR angiographic technique that allows visualization of the proximal and distal portions of the renal arteries without the use of contrast media during free breathing. To obtain high contrast and high spatial resolution, a cardiac-triggered navigator-gated free-breathing 3D steady-state free-precession (SSFP) sequence was employed in conjunction with a slab-selective inversion prepulse. Initial results of this novel approach are presented.

METHODS

Study population

MRA of the renal arteries was performed in eight clinically healthy volunteers (4 men and 4 women, mean age 29 years) with no history of hypertension, cardiovascular, or renal disease. Subsequently, eight consecutive patients (5 men and 3 women, mean age 53 years, blood pressure $152 \pm 16/94 \pm 12$ mm Hg, creatinine 1.6 ± 0.9 mg/dL, urea 55.4 ± 46.2 mg/dL) with hypertension and suspected renovascular disease, who were referred to the department of radiology for diagnostic imaging of the renal arteries were investigated.

The study protocol was approved by the institutional review board, and all subjects gave informed consent prior to inclusion into the study.

MR imaging

All examinations were carried out on a commercial 1.5 T whole-body MR system (ACS-NT; Philips Medical Systems, Best, The Netherlands) equipped with a commercial cardiovascular software package (Inca; Philips Medical Systems, Best, The Netherlands) and a high-performance gradient system (PowerTrak® 6000; Philips Medical Systems, Best, The Netherlands). A five-element synergy coil was used for signal reception.

Scout imaging

Initially, coronal, sagittal, and transverse multistack SSFP scout images were acquired [repetition time (TR)/echo time (TE) 3.8/1.9 ms, excitation angle 55°, field of view 450 × 450 mm^2, matrix 128 × 128, number of slices and slice thickness: nine 10-mm thick slices each stack, scanning time 7 seconds] to localize the abdominal aorta, the ostia of the renal arteries, the kidneys, and the dome of the right diaphragm.

Phase-contrast MR angiography

In all volunteers and patients, a diastolic triggered 3D phase-contrast MRA (pcMRA)[14] was first performed (TR/TE 20/7 ms, excitation angle 20°, field of view 170 × 120 mm^2, matrix 128 × 90, in-plane resolution 1.3 × 1.9 mm^2, reconstructed to 0.6 × 0.6 mm^2 using a 256 × 256 matrix, number of slices and slice thickness: 20 3.0-mm thick slices, interpolated to 40 1.5-mm thick slices) using peripheral pulse unit gating with an acquisition window of 394 ms, resulting in a scanning time of nine minutes and nine seconds for a heart rate of 70 beats per minute. Slices in the transverse orientation were acquired, and maximum intensity projections (MIPs) in the transverse plane were calculated.

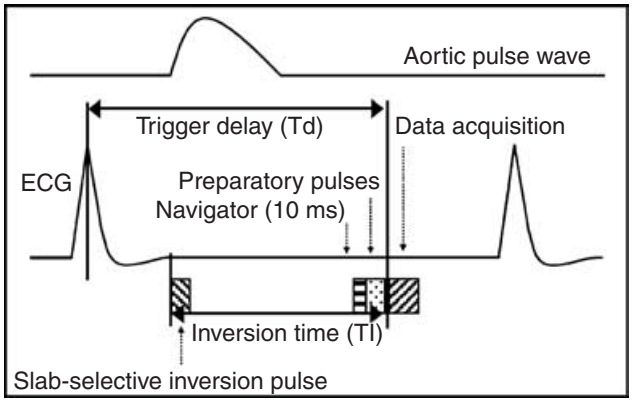

Fig. 1. Schematic of the sequence elements for cardiac-triggered navigator-gated steady-state free-precession (SSFP) renal MRA. Trigger delay time (Td) was individually adjusted in order to apply the inversion prepulse before, and data acquisition after, the pulsatory wave. Using an inversion delay time of 325 ms, signal of the renal parenchyma and the venous blood were suppressed. The real-time navigator precedes the preparatory pulses, which are used to reach steady-state conditions.

Contrast-enhanced MR angiography

In all patients 3D contrast-enhanced MR angiograms (ceMRA) were obtained for comparison (TR/TE 3.7/1.1 ms, excitation angle 40°, field of view 500 × 350 mm^2, matrix 512 × 154, in-plane spatial resolution 1.0 × 2.6 mm^2, reconstructed to 1.0 × 1.0 using a 512 × 512 matrix, number of slices and slice thickness: 23 3-mm thick slices, interpolated to 46 1.5-mm thick slices, scanning time 11 seconds). Gadopentetate dimeglumine (0.2 mmol per kg of body weight, Magnevist®; Schering, Berlin, Germany) was administered intravenously.

SSFP inversion recovery MR angiography

A cardiac-triggered navigator-gated SSFP sequence (TR/TE 4.4/2.2, excitation angle 85°, field of view 320 × 320 mm^2, matrix 256 × 256, in-plane spatial resolution 1.25 × 1.25 mm^2, reconstructed to 0.6 × 0.6 mm^2 using a 512 × 512 matrix) was used for free-breathing renal MRA (Fig. 1). The acquired 3D volume included 10 4.0-mm thick sections that were interpolated (with 0 filling) to 20 contiguous 2.0-mm thick slices. In order to achieve steady-state conditions 20 repetitive radiofrequency excitations were performed as dummy cycles for each cardiac cycle interval immediately before data acquisition [15]. Using a slab-selective inversion prepulse (ss Inv SSFP)

with an appropriate inversion time (TI) signal of the static, tissue was suppressed depending on the specific relaxation time, while inflowing blood, which washes into the imaging volume during the TI, maintains high signal intensity. In the volunteer group, different TIs (275 to 400 ms) were used to determine the optimal inversion delay, in which the signal of the renal parenchyma, as well as the blood in the veins, is equally suppressed. In addition, in the volunteer group, the same sequence was repeated with a non–slab-selective inversion pulse (non-ss Inv SSFP) and without magnetization preparation (no Inv SSFP). Based on the volunteer data, for the patient study a TI of 325 ms was used. Trigger delay time (Td) was adjusted in order to apply the inversion pulse prior to systole and the readout pulse at diastole. Hereby, 32 radiofrequency excitations were acquired in each cardiac cycle interval. With such timing, high spatial-resolution MR images can be obtained, eliminating motion and diameter changes in the proximal renal arteries, which occur in untriggered sequences due to the aortic pulse wave [10]. The higher blood flow during systole supports the wash-in of unsaturated blood. For accurate targeting of the renal arteries, double-oblique section orientations were planed using a three-point plan scan tool [16].

For suppression of respiratory motion artifacts, prospective real-time navigator technology was used, which allowed data acquisition during free breathing as previously described [13, 17]. Hereby, the user-specified gating window was set to 5 mm, which resulted in navigator efficiency higher than 50% as previously described [17] and in all investigated subjects in our series. For a heart rate of 70 beats per minute, the examination duration (including the navigator gating) ran up to approximately 3 minutes.

On the whole, three local presaturation bands were used. Two of them were placed ventrally to suppress signal from the intestine and the ventrolateral abdominal wall. A third one was positioned caudally to suppress signal from inflowing blood of the inferior vena cava [18]. Additionally, a shim volume was positioned including the aorta and the renal arteries. The phase encoding direction was set to right-left to avoid motion artifacts originating from the bowel.

Data analysis

Signal intensities (SI) were measured in user-specified regions of interest (ROI) that were placed in the aorta (ao), the proximal-middle portion of the renal arteries (ra), as well as of the renal veins (rv), renal parenchyma (ki), and the adjacent soft tissue represented by the paravertebral muscle (st). The ROIs with identical size and position were placed in all three sequences (ss Inv SSFP, no Inv SSFP, and non-ss Inv SSFP). Afterwards, signal-to-noise ratio (SNR) and contrast-to-noise ratio (CNR) were compared. SNR of the aorta, the renal arteries, and veins were calculated as $SNR_{ROI} = SI_{ROI}/SD_{ROIa}$, where SD_{ROIa} is the standard deviation of the signal in a region of air. CNR were calculated as $CNR_{ra\text{-}rv} = (SI_{ROIra}–SI_{ROIrv})/SD_{ROIa}$, $CNR_{ra\text{-}ki} = (SI_{ROIra}–SI_{ROIki})/SD_{ROIa}$, and $CNR_{ra\text{-}st} = (SI_{ROIra}–SI_{ROIst})/SD_{ROIa}$. In the patient study, images obtained from the new SSFP sequence with the slab-selective inversion pulse and from ceMRA were compared. However, because the position of the renal veins cannot be clearly located in ceMRA, only SNR of the aorta and renal arteries, as well as the CNR between renal arteries and parenchyma or paravertebral soft tissue, respectively, were calculated.

Images obtained from patients using ss Inv SSFP, pcMRA, and ceMRA were assessed in terms of image quality by two investigators (E.S. and M.K.) blinded to sequence parameters on a three-grade scale (1 = good image quality with sharply defined renal arteries, 2 = reduced image quality but renal arteries still visible, 3 = poor image quality without sufficient visualization of the renal arteries). Additionally, all renovascular findings (like stenosis grade) in ss Inv SSFP MRA were compared to ceMRA (A.B. and M.K.). In three patients additional x-ray angiograms were available for comparison.

Maximal visible vessel length was measured in the maximum intensity projection (MIP) reconstructions of the ss Inv SSFP MRA, pcMRA, and ceMRA.

Statistical analysis

The results were expressed as mean ± 1 SD, and statistical differences between the sequences were analyzed for significance by the nonparametric Wilcoxon test for objective image quality parameters using JMP (JMP Discovery Software 5.0.1.2; Cary, NC, USA). Differences between groups with at least $P < 0.008$ were considered to be statistically significant according to the method of Holm-Bonferroni [19].

RESULTS

Using ss Inv SSFP renal MRA, high signal intensity could be achieved in the aorta as well as in the renal arteries, including the more distal braches, while the signal of the renal veins and renal parenchyma was almost completely suppressed (Fig. 2A). However, in some cases the inferior caval vein could be delineated ventrally to the right renal artery with intermediate signal. The effect of the slab-selective inversion prepulse is demonstrated when no magnetization prepulse or a non–slab-selective inversion prepulse was applied. As demonstrated in Figure 2B, a high signal intensity of all vessels, including the veins and the surrounding tissue, occurs if no inversion pulse is applied. As a result, small branches cannot be depicted because of the increasing signal intensity of

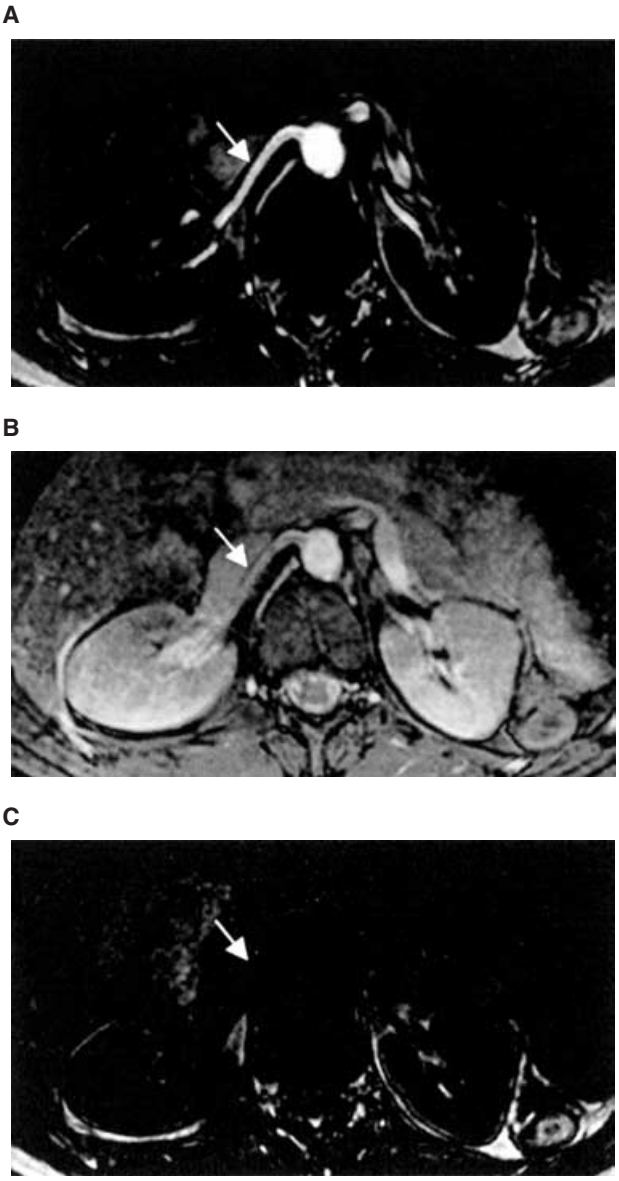

Fig. 2. Single slice images demonstrating the effect of a slab-selective inversion pulse (*A*), no inversion pulse (*B*), and a non–slab-selective inversion pulse (*C*).

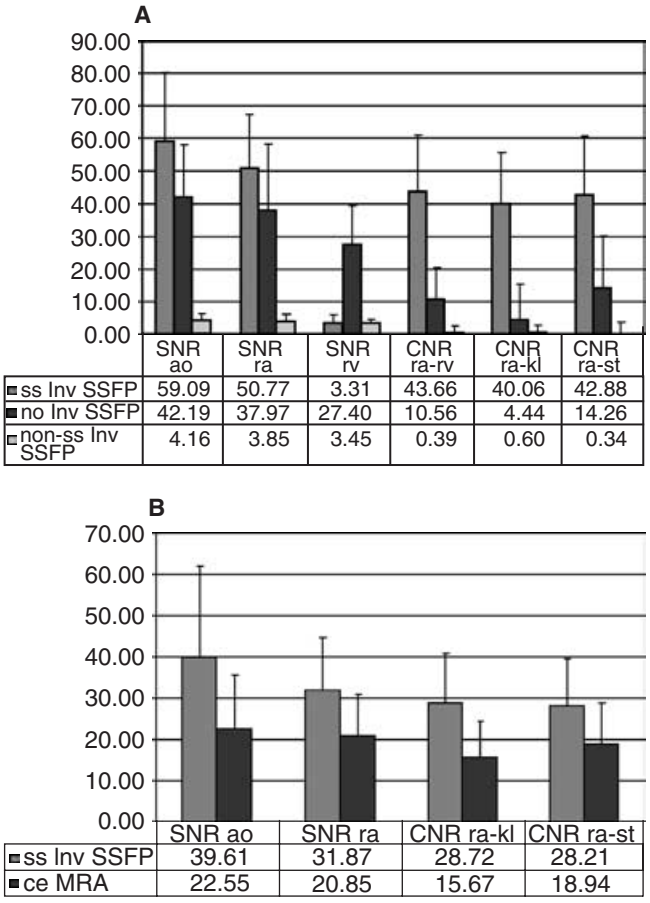

Fig. 3. Signal-to-noise ratio (SNR) and contrast-to-noise ratio (CNR) calculated from the aorta (ao), renal artery, and vein (ra, rv), parenchyma of the kidney (ki), and soft tissue (st). In the volunteer study, SNR and CNR in steady-state free-precession (SSFP) images with a slab-selective inversion pulse (ss Inv SSFP), without magnetization preparation (no Inv SSFP), and with a non–slab-selective inversion pulse (non-ss Inv SSFP) were compared (*A*). In the patient study, SNR and CNR in SSFP imaging with a slab-selective inversion pulse and ceMRA were compared (*B*).

the renal parenchyma. Larger arteries are difficult to distinguish from veins. In comparison, neither arteries nor veins were visible using a non–slab-selective inversion pulse (Fig. 2C).

SNR and CNR data in the volunteer study are shown in Figure 3A. Statistically significant higher SNR for both aorta and renal arteries were found in ss Inv SSFP imaging (aorta 60 ± 21; renal artery 51 ± 16) compared with no Inv SSFP (aorta 42 ± 16; renal artery 38 ± 20), and particularly to non-ss Inv SSFP imaging (aorta 4 ± 2; renal artery 4 ± 2), $P < 0.008$. The two latter sequences yielded a low contrast between the renal arteries and the veins (11 ± 9 and 0 ± 2). In contrast to this, a significantly improved CNR between the renal arteries and the renal veins was observed (44 ± 17; $P < 0.008$) if a slab-selective inversion pulse was used. The good suppression of the static tissue led also to an increased contrast between arteries and renal parenchyma, as well as the surrounding tissue, such as the paravertebral muscle (Fig. 3A).

The proximal, middle, and distal portion, including the segmental arteries and branches embedded in the parenchyma, could be clearly visualized in all volunteers using ss Inv SSFP MRA. A representative MIP image is shown in Figure 4 alongside a MIP of a pcMR angiogram for comparison. The maximal visible vessel length on ss Inv SSFP images of the volunteers was 79 and 71 mm on average for the right and left renal artery, respectively. The measurable vessel length using ss Inv SSFP images were comparable with the vessel length obtained from images using pcMRA (right 83 mm, left 67 mm). The measurable vessel length from patients was more limited compared with the volunteer study (right 58 mm, left

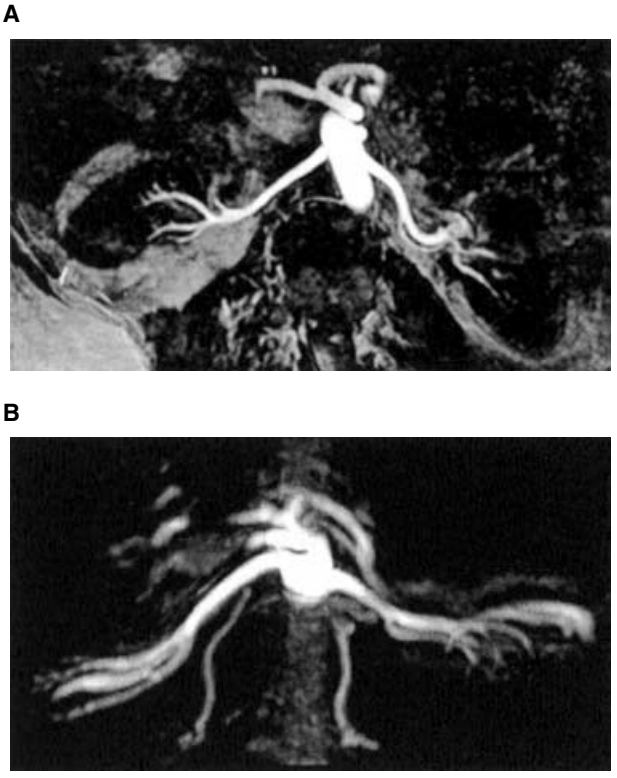

Fig. 4. Maximum intensity projections of a ss Inv steady-state free-precession (SSFP) magnetic resonance angiography (MRA) (*A*) and phase-contrast MRA (pcMRA) (*B*). Note that in SSFP imaging, respiratory and cardiac motion is almost completely suppressed due to navigator-gating and cardiac-triggering resulting in sharp delineation of the vessel lumen.

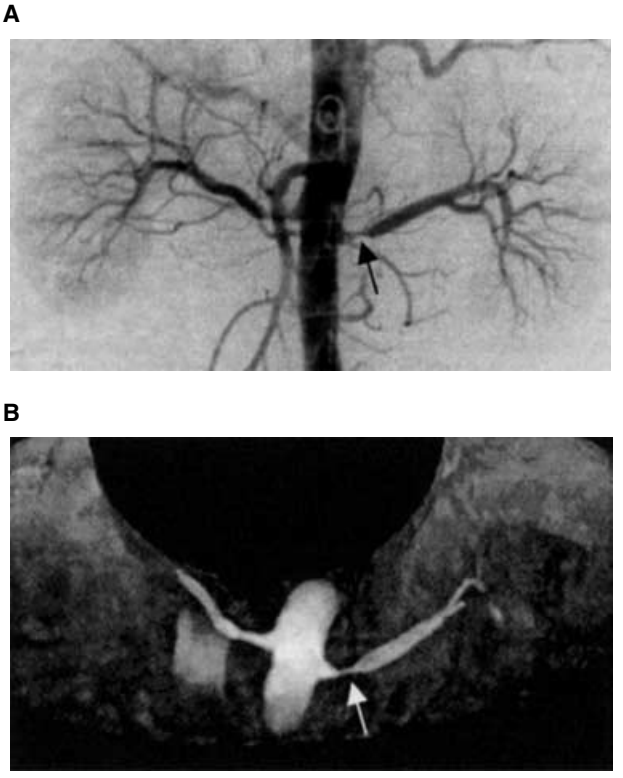

Fig. 5. Conventional x-ray angiography in a patient with renovascular hypertension (150/110 mm Hg) demonstrating a high-grade stenosis of the left renal artery (*A*). Although quality of the ss Inv steady-state free-precession (SSFP) maximum intensity projections (MIP) image is relatively poor, the stenosis of the left renal artery (arrow) could be clearly determined without signal void distal to the stenosis (*B*). The distal portion of the right renal artery is outside the slices used for maximum intensity projection for the left renal artery.

45 mm). However, using pcMR angiography (right 62 mm, left 50 mm), and even the use of the ceMR angiography (right 54 mm, left 49 mm) yielded similar average values concerning the visible vessel length (NS). However, in pcMRA, as well as ceMRA especially, the distal branches of the renal arteries appeared more blurred, as can be seen in Figure 4. In the patient study, all SNRs and CNRs obtained from ss Inv SSFP images demonstrated superior values compared to ceMRA (Fig. 3B). Subjective image quality was also superior in ss Inv SSFP imaging (1.4 ± 0.5) compared to pcMRA (2.0 ± 0.9) or ceMRA (1.6 ± 0.8); however, the differences did not reach statistical significance. In four out of eight patients, renal arteries with stenotic lesions were found. All low-grade ($N = 3$) as well as high-grade ($N = 3$) stenoses determined by ss Inv SSFP angiograms could be verified by ceMRA or conventional x-ray angiography (Fig. 5). In addition, one patient with a single kidney on the left side was correctly identified (Fig. 6).

DISCUSSION

In this study, a novel SSFP MR sequence was established with a slab-selective inversion prepulse for selective renal MRA.

The SSFP technique was used because previous studies demonstrated that in addition to a high SNR, this sequence bears intrinsically high (T_2-like) contrast between the blood pool and soft tissue [13, 20]. SSFP imaging is supposed to be flow compensated in all three spatial coordinates due to the symmetric shape of the gradient pulses [20]. Neither in-flow– nor out-flow–related artifacts [21] could be observed in our study, which may be a result of a thin volume thickness, sufficient shimming using a volume shim, and adequate timing with data acquisition in diastole.

The application of a slab-selective inversion prepulse as used in this study resulted in a good signal suppression of static tissue and veins, which allowed the selective visualization of the renal arteries without the use of any contrast medium application. The TI of 325 ms, which was chosen empirically from the volunteer study, proved to be concordant with the mean null crossing of the renal parenchyma (300 ms) and the blood (350 ms) calculated using Fleckenstein's formula (based on a T_1 relaxation time of 650 ms for the renal parenchyma and 1200 ms for the blood for a heart rate of 70 per minute)[22]. The

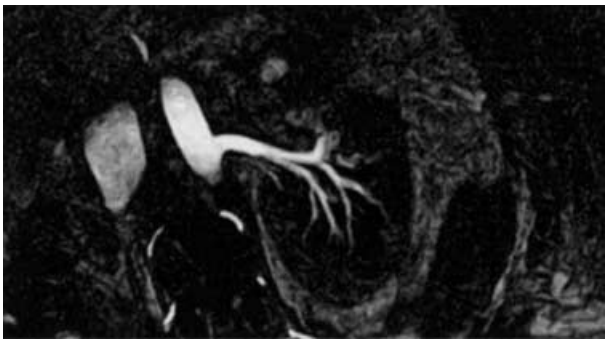

Fig. 6. Steady-state free-precession (SSFP) imaging with a slab-selective inversion prepulse in a patient with hypertension and suspected renovascular disease demonstrating a single kidney on the left side without stenosis (MIP). MIP, maximum intensity projection.

heart rate depending adjustment of the TI may further improve the signal suppression of the surrounding tissue in future examinations.

Our preliminary data in patients indicate the potential for correct determination of all renal artery stenoses. Even for high-grade stenoses no signal void was observed distal to the stenoses, which would impair the correct estimation (Fig. 5). This limitation reduces the clinical value of other non–contrast-enhanced sequences like time-of-flight and pcMRA.

The presented renal MRA technique is equipped with ECG-triggering, navigator technology, and double-oblique targeting of the renal vessels, which may lead to a slightly increased preparation and planning durations. However, using ECG-triggering, all the tissue and blood within the target plane receives the inversion pulse before systole. The subsequent inflow of spins in the renal arteries during systole supports the blood exchange for MRA. By collecting data during diastole, pulsatile flow artifacts and motion artifacts of the proximal renal arteries that originate from the aortic pulse wave are minimized [10]. A relatively brief acquisition window in late diastole enables for high temporal resolution imaging with further reduction of motion artifacts. Furthermore, end-expiratory navigator gating of the right hemi-diaphragm provided sufficient respiratory motion suppression despite the large displacement of the distal renal arteries during the normal respiratory cycle [9, 23]. Due to the use of free-breathing navigator technology there is no time constraint, which facilitates data acquisition for increased spatial resolution even in patients with reduced breath-hold capability. The examination time for the presented sequence accounts for approximately three minutes, which is long compared with ceMRA, where only one breath-hold is needed. However, the scanning time in our approach is much faster (about four times) than former navigator-gated free-breathing approaches [13]. The longer image acquisition time compared with ceMRA is invested into improved spatial resolution and reduction of motion artifacts arising from the pulse wave and breathing. Another drawback of ceMRA is that only one data acquisition can be performed, although this limitation is not seen in our approach. Unfortunately, a relatively low spatial resolution was used in all sequences (including ceMRA) due to the lack of parallel imaging techniques on the scanner at the time of our study. However, in future studies, the combination of the ss Inv SSFP sequence and parallel imaging techniques like simultaneous acquisition of spatial harmonics (SMASH) [24] or sensitivity encoding (SENSE) [25] is also conceivable to further reduce scanning time or to improve spatial resolution.

Due to the variable anatomic orientation of the right and left kidneys, axial slab orientation for renal MRA can be suboptimal. This may be overcome by acquiring larger 3D slabs, or by volume targeting of a slab that closely encompasses both renal arteries. In our study, we chose to use a three-point plan scan tool [16], which allowed individual adaptation of double-oblique section orientations parallel to both renal arteries. Consequently, renal arteries, including more distal portions, could be imaged with a thinner slab, consistent with a reduced imaging time and minimized blood saturation in the abdominal aorta.

CONCLUSION

The combination of an ECG-triggered, navigator-gated, 3D SSFP sequence and a slab-selective inversion prepulse enables selective MRA of the renal arteries and its branches during free breathing. Due to the relatively short scanning time and the high signal, as well as high contrast visualization of the renal arteries without contrast media, this sequence may provide a promising screening technique for patients suspected of having renovascular disease. No special software or hardware is required; thus, the implementation of this sequence should be possible on most currently installed MR systems. The renal MRA technique used in this study was performed with healthy volunteers and a small group of patients. Our preliminary patient data, however, demonstrate high clinical promise for this approach and warrants larger patient comparison studies, including patients with renovascular disease defined by ceMRA or conventional x-ray angiography.

Reprint requests to Marcus Katoh, M.D., Department of Diagnostic Radiology, University Hospital, University of Technology (RWTH), Pauwelsstrasse 30, 52057 Aachen, Germany.
E-mail: katoh@rad.rwth-aachen.de

REFERENCES

1. Nishimura DG: Time-of-flight MR angiography. *Magn Reson Med* 14:194–201, 1990
2. Li D, Haacke EM, Mugler JP 3rd, *et al*: Three-dimensional time-of-flight MR angiography using selective inversion recovery RAGE

with fat saturation and ECG-triggering: Application to renal arteries. *Magn Reson Med* 31:414–422, 1994
3. Dumoulin CL, Cline HE, Souza SP, *et al*: Three-dimensional time-of-flight magnetic resonance angiography using spin saturation. *Magn Reson Med* 11:35–46, 1989
4. Dumoulin CL, Souza SP, Walker MF, *et al*: Three-dimensional phase contrast angiography. *Magn Reson Med* 9:139–149, 1989
5. Prince MR, Schoenberg SO, Ward JS, *et al*: Hemodynamically significant atherosclerotic renal artery stenosis: MR angiographic features. *Radiology* 205:128–136, 1997
6. Prince MR: Gadolinium-enhanced MR aortography. *Radiology* 191:155–164, 1994
7. Grist TM: Magnetic resonance angiography of renal arterial stenosis. *Coron Artery Dis* 10:151–156, 1999
8. Maki JH, Chenevert TL, Prince MR: Contrast-enhanced MR angiography. *Abdom Imaging* 23:469–484, 1998
9. Vasbinder GB, Maki JH, Nijenhuis RJ, *et al*: Motion of the distal renal artery during three-dimensional contrast-enhanced breath-hold MRA. *J Magn Reson Imaging* 16:685–696, 2002
10. Kaandorp DW, Vasbinder GB, de Haan MW, *et al*: Motion of the proximal renal artery during the cardiac cycle. *J Magn Reson Imaging* 12:924–928, 2000
11. Edelman RR, Siewert B, Adamis M, *et al*: Signal targeting with alternating radiofrequency (STAR) sequences: Application to MR angiography. *Magn Reson Med* 31:233–238, 1994
12. Wielopolski PA, Adamis M, Prasad P, *et al*: Breath-hold 3D STAR MR angiography of the renal arteries using segmented echo planar imaging. *Magn Reson Med* 33:432–438, 1995
13. Spuentrup E, Manning WJ, Bornert P, *et al*: Renal arteries: Navigator-gated balanced fast field-echo projection MR angiography with aortic spin labeling. Initial experience. *Radiology* 225:589–596, 2002
14. de Haan MW, Kouwenhoven M, Thelissen RP, *et al*: Renovascular disease in patients with hypertension: Detection with systolic and diastolic gating in three-dimensional, phase-contrast MR angiography. *Radiology* 198:449–456, 1996
15. Spuentrup E, Bornert P, Botnar RM, *et al*: Navigator-gated free-breathing three-dimensional balanced fast field echo (TrueFISP) coronary magnetic resonance angiography. *Invest Radiol* 37:637–642, 2002
16. Stuber M, Botnar RM, Danias PG, *et al*: Double-oblique free-breathing high resolution three-dimensional coronary magnetic resonance angiography. *J Am Coll Cardiol* 34:524–531, 1999
17. Stuber M, Botnar RM, Danias PG, *et al*: Submillimeter three-dimensional coronary MR angiography with real-time navigator correction: Comparison of navigator locations. *Radiology* 212:579–587, 1999
18. Prasad PV, Kim D, Kaiser AM, *et al*: Noninvasive comprehensive characterization of renal artery stenosis by combination of STAR angiography and EPISTAR perfusion imaging. *Magn Reson Med* 38:776–787, 1997
19. Holm S: A simple sequentially rejective multiple test procedure. *Scandinavian Journal of Statistics* 6:65–70, 1979
20. Duerk JL, Lewin JS, Wendt M, *et al*: Remember true FISP? A high SNR, near 1-second imaging method for T2-like contrast in interventional MRI at .2 T. *J Magn Reson Imaging* 8:203–208, 1998
21. Markl M, Alley MT, Elkins CJ, *et al*: Flow effects in balanced steady state free precession imaging. *Magn Reson Med* 50:892–903, 2003
22. Fleckenstein JL, Archer BT, Barker BA, *et al*: Fast short-tau inversion-recovery MR imaging. *Radiology* 179:499–504, 1991
23. Schwartz LH, Richaud J, Buffat L, *et al*: Kidney mobility during respiration. *Radiother Oncol* 32:84–86, 1994
24. Sodickson DK, Manning WJ: Simultaneous acquisition of spatial harmonics (SMASH): Fast imaging with radiofrequency coil arrays. *Magn Reson Med* 38:591–603, 1997
25. Pruessmann KP, Weiger M, Scheidegger MB, *et al*: SENSE: Sensitivity encoding for fast MRI. *Magn Reson Med* 42:952–962, 1999